Research on Engineering Structures & Materials
www.jresm.org
Research Group

Research Article

Analytical solutions for the deformation calculation of compressive pile group incorporating reinforcement and shadowing effects

Shangping Chen [*,1,2,a], Huacong Zhou [*,3,b], Guoxi Che [4,c], Lijun Yan [5,d], Hongjuan Qu [1,e], Yuxin Zheng [1,6,f], Wenjuan Yao [7,g], Jiachen Zhao [1,h], Yanhui Wu [1,i]

[1]*School of Civil Engineering and Architecture, Zhejiang Guangsha Vocational and Technical University of Construction, Dongyang, Zhejiang, China*
[2]*Zhejiang Society for Geotechnical Mechanics & Engineering, Ningbo, Zhejiang, China*
[3]*School of Architecture and Civil Engineering, Anhui Polytechnic University, Wuhu, Anhui, China*
[4]*Zhejiang Provincial Geology and Mineral Construction Co., Ltd., Hangzhou, Zhejiang, China*
[5]*School of Environmental Science and Engineering, Shanghai Jiao Tong University, Shanghai, China*
[6]*School of Civil Engineering and Architecture, Zhejiang University of Science and Technology, Hangzhou, Zhejiang, China*
[7]*Shanghai Institute of Applied Mathematics and Mechanics, Shanghai University, Shanghai, China*

Article Info

Article History:

Received 20 June 2026

Accepted 29 Aug 2026

Keywords:

Compressive pile group;
Reinforcement and shadowing effects;
Interaction coefficient;
Deformation;
Analytical solutions

Abstract

This study addresses the deficiency in existing research on the deformation calculation of compressive pile groups, which often overlooks the Reinforcement and Shadowing Effects (RSE) among piles. The concept of RSE within pile groups is redefined, and an in-depth investigation is conducted on the deformation calculation theory incorporating RSE. By leveraging the shear deformation mechanism of coaxial cylindrical shells and the principle of elastic superposition, a calculation method and corresponding analytical solution for the deformation of compressive piles considering RSE in pile groups are established and derived. The validity of the proposed calculation model is verified by comparing it with measured field data and finite element simulation results. This method overcomes the limitations of existing approaches that fail to adequately account for the mutual RSE among piles in a group, thereby more accurately reflecting the actual mechanical behavior of pile groups and enabling deformation analysis for large-scale pile groups. Furthermore, we investigate the relationship between key parameters, such as the length-diameter ratio, spacing-diameter ratio, pile-soil modulus ratio, and soil Poisson's ratio, and the deformation of pile group through dimensional analysis and parameter influence studies. The proposed methodology not only enhances the accuracy of deformation predictions but also offers valuable insights for the design, construction, and monitoring of pile foundations in engineering practice.

© 2026 MIM Research Group. All rights reserved.

1. Introduction

In recent years, with the continuous advancement of construction technology for high-rise buildings, pile group foundations, as an essential form of deep foundation, have been increasingly widely adopted in various engineering projects. By focusing on the bearing performance, field and model tests, and deformation characteristics of compression pile group, research conducted by

*Corresponding author: shangping_chen@shu.edu.cn; huacong@ahpu.edu.cn
[a]orcid.org/0000-0001-5921-3121; [b]orcid.org/0009-0009-3085-9952; [c]orcid.org/0009-0004-6441-1199; [d]orcid.org/0000-0001-9393-5822; [e]orcid.org/0009-0006-2743-7116; [f]orcid.org/0009-0004-9329-1675; [g]orcid.org/0009-0007-7105-7505; [h]orcid.org/0009-0007-2916-9300; [i]orcid.org/0009-0007-5227-5515
DOI: http://dx.doi.org/10.17515/resm2026-1767me0620rs

numerous scholars [1-16] worldwide has yielded remarkable progress in experimental investigation, numerical simulation and theoretical analysis.

Nevertheless, the objectively existing RSE among piles results in diverse and complex influencing factors for the mechanical and deformation responses of pile group, leaving the research on pile group deformation calculation lagging behind engineering practice. The complexity of pile group deformation fundamentally originates from the unique RSE. Specifically, the interaction between adjacent piles through surrounding soils forms a complicated three-dimensional mechanical system. Establishing a rational calculation model that can accurately reflect this complex interaction mechanism and balance calculation accuracy and efficiency has long been a core scientific issue in geotechnical engineering over the past decades.

Scholars at home and abroad have conducted extensive research on the deformation of compression pile group and developed a variety of calculation theories and methods: (1) The equivalent pier foundation method specified in current codes, such as Chinese national code Technical Code for Building Pile Foundations (JGJ 94-2008) [17], simplifies the pile group into a solid deep foundation with a certain size and calculates settlement based on conventional deep foundation deformation theories; (2) The elastic theory method represented by Poulos and Davis [18,19] is one of the most widely applied and well-developed theoretical approaches. Based on Mindlin's elastic stress solution, this method introduces pile–pile interaction factors to linearly superimpose the additional settlement induced by adjacent piles, so as to obtain the overall settlement of pile group; (3) The shear displacement method proposed by Randolph et al. [20]. simplifies the displacement field of pile-side soils, establishes a single-pile deformation model based on the load transfer theory, and is further extended to pile group analysis via the superposition principle; (4) Numerical methods [21-25], including the three-dimensional finite element method (FEM), finite difference method (FDM) and discrete element method (DEM), serve as the most refined tools for simulating the mechanical and deformation behavior of pile group; (5) Other analytical approaches [26,27], such as the boundary element method advocated by Butterfield, the hybrid method developed by Chow, and the variational analysis method for pile group proposed by Shen, have provided valuable insights into pile group analysis from different perspectives.

While the aforementioned methods have significantly advanced the theoretical research and engineering application of pile group analysis, they share a prominent common limitation: the pile-pile interaction is treated primarily through unidirectional displacement superposition or empirical correction, without separating the intrinsic Reinforcement Effect from the Shadowing Effect. In essence, the core bottleneck restricting further progress in current pile group deformation calculation research is the inability to thoroughly disclose and quantitatively quantify the underlying physical mechanism of RSE. To this end, it is still challenging to propose an innovative analytical model that possesses rigorous theoretical foundation, favorable computational efficiency and strong practical engineering applicability.

Against the above research background, this paper conducts an in-depth study on the deformation theory of pile group considering the RSE, and proposes a novel analytical method fully incorporating pile-group RSE. By adopting a simplified mechanical model and reasonable boundary conditions, an analytical solution for pile group deformation considering mutual RSE interaction is derived. The proposed method greatly improves the efficiency, rationality and practicability of pile group deformation calculation, and can provide a novel and effective theoretical support for the design and analysis of large-scale complex pile group.

2. Analysis Model of RSE

2.1. Deformation Analysis Considering RSE

When a pile settles under loading, it induces changes in the deformation and stress fields of the surrounding soil. These changes propagate to adjacent piles, inducing additional deformation in neighbouring piles, which is equivalent to applying additional loads on them; and vice versa. This mutual reinforcing and shadowing effect transmitted through the soil medium is defined as the RSE

in this paper. The mutual interaction coefficient will be employed to quantitatively analyse this effect.

As shown in Fig. 1, the pile group is situated in uniform soil. All piles in the group share identical properties in terms of material, diameter, and depth, as shown below:

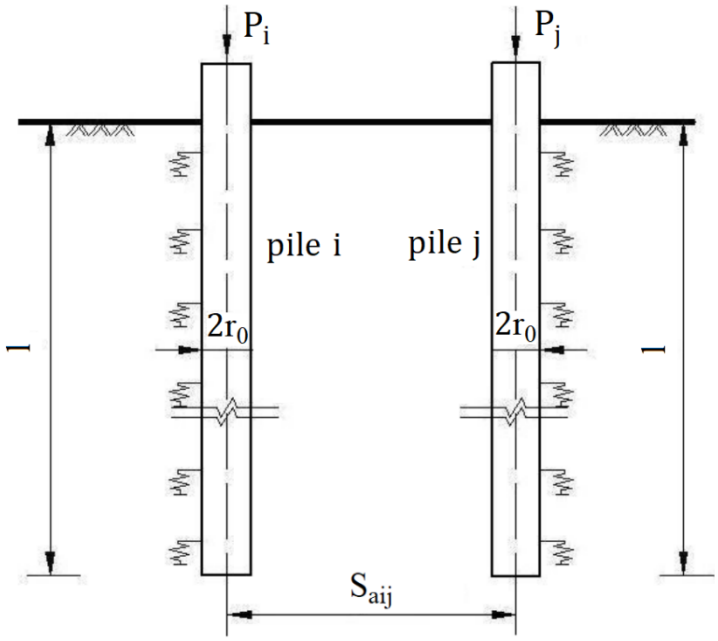


Fig. 1. Schematic diagram of compressive pile group

For axially loaded pile group foundations, the composition of vertical deformation for an arbitrary pile (pile i or pile j) is analyzed as follows:

- When vertical load P_i is applied at the pile top of pile i and pile j does not exist, pile i generates its own active vertical deformation S_{ii};
- When pile i is in an unloaded state and vertical load P_j acts on the pile top of pile j, the reinforcement effect of pile j on pile i is considered. The active deformation S_{jj} of pile j will induce passive vertical deformation S_{ij} in pile i. The calculation method of S_{jj} is identical to that of S_{ii};
- When vertical load P_i is applied at the pile top of pile i and pile j is unloaded, the reinforcement effect of pile i on pile j is considered. The active deformation S_{ii} of pile i will induce passive vertical deformation S_{ji} in pile j. Meanwhile, the shadowing effect of pile j on pile i will produce an attenuation deformation S_{ij1} against the active deformation S_{ii} of pile i, and the actual deformation of pile i is S_{ii}^*. In addition, the shadowing effect of pile i on pile j will produce an attenuation deformation S_{ji1}^* against the passive deformation S_{ji} of pile j, resulting in the actual passive deformation S_{ji}^* of pile j;
- For the condition (2) above, the shadowing effect of pile i on pile j will produce an attenuation deformation S_{ji1} against the active deformation S_{jj} of pile j, and the actual deformation of pile j is S_{jj}^*. Meanwhile, the shadowing effect of pile j on pile i will produce an attenuation deformation S_{ij1}^* against the passive deformation S_{ij} of pile i, resulting in the actual passive deformation S_{ij}^* of pile i.

According to the above deformation analysis, the final deformation of pile i in the axially loaded pile group is given by:

$$S_i(z)=S_{ii}^*(z)+\sum_{j=1,j\neq i}^{n} S_{ij}^*(z) \quad (1)$$

Where;

$$S_{ii}^{*}(z)=S_{ii}(z)-S_{ij1}(z) \tag{2}$$

$$S_{ij}^{*}(z)=S_{ij}(z)-S_{ij1}^{*}(z) \tag{3}$$

Similarly, the final settlement of pile j in the axially loaded pile group is expressed as:

$$S_{j}(z)=S_{jj}^{*}(z)+\sum_{i=1,i\neq j}^{n} S_{ji}^{*}(z) \tag{4}$$

where

$$S_{jj}^{*}(z)=S_{jj}(z)-S_{ji1}(z) \tag{5}$$

$$S_{ji}^{*}(z)=S_{ji}(z)-S_{ji1}^{*}(z) \tag{6}$$

Analysis of the deformation components of pile i and pile j in the aforementioned pile group demonstrates that mutual reinforcement effect and shadowing effect exist between pile i and pile j during the deformation process. Existing calculation methods for pile group deformation fail to fully consider this factor. Based on the fundamental previous research achievements of our research group [28-33], this paper carries out research on this key scientific issue and solves it.

2.2. Interaction Coefficient Considering RSE

Here, the interaction coefficient ξ_{ij} is introduced. Its physical meaning is as follows: Under the loading condition of "pile i is present with no load on its top, and the load on the top of pile j is P_j", considering the interaction between pile i and pile j, the ratio of the deformation of pile i to that of pile j at the same depth is denoted as $\xi_{ij}=S_{ij}^{*}/S_{jj}^{*}$. The deduction of ξ_{ij} is presented below.

Under the loading condition where "pile i is present with no load on its top, and the load on the top of pile j is P_j", when a compressive load acts on pile j, a lateral frictional resistance $\tau_{j0}(r_0)$ is generated. The deformation field of the soil mass surrounding pile j can be described as follows:

$$\left.\begin{array}{ll} S_{jj}(z) & =\frac{\tau_{j0}(r_0)r_0}{G_s} ln\left(\frac{r_m}{r}\right) \quad (r<r_m) \\ S_{jj}(z) & =0 \quad (r\geq r_m) \end{array}\right\} \tag{7}$$

The soil deformation field expression in formula (7) follows the single-pile shear displacement derivation framework proposed by Randolph and Wroth (1979) [20], which is extended to group-pile mutual interaction analysis in this work.

Based on the studies conducted by Poulos (1980) [18] and Randolph et al. (1979) [20], the mathematical expression of r_m is given by:

$$r_m=2.5(1-\nu_s)l \tag{8}$$

where ν_s is the Poisson's ratio of the soil around the pile, and l is the embedment depth of the pile.

Based on formula (7), the deformations at a depth of z for pile j and pile i induced by $\tau_{j0}(r_0)$ are respectively:

$$\left.\begin{array}{ll} S_{jj}(z) & =\frac{\tau_{j0}(r_0)r_0}{G_s} ln\left(\frac{r_m}{r_0}\right) \quad (r\leq r_m) \\ S_{ij}(z) & =\frac{\tau_{j0}(r_0)r_0}{G_s} ln\left(\frac{r_m}{S_{aij}}\right) \quad (r\leq r_m) \end{array}\right\} \tag{9}$$

In accordance with the shear deformation mechanism of coaxial cylindrical shells [19,20,32], the lateral frictional resistance at the location of pile i induced by τ_{j0} can be formulated as:

$$\tau_{ij} = \frac{\tau_{j0}(r_0) r_0}{S_{aij}} \tag{10}$$

Meanwhile, due to the mutual shadowing effect between pile i and pile j, this effect respectively restrains the surrounding soil of pile j and pile i from further shear deformation. This passive action induces a corresponding attenuation displacement at the positions of pile i and pile j, respectively:

$$\left.\begin{aligned} S^*_{ij1}(z) &= \frac{r_0\tau_{j0}}{G_s}\frac{r_0}{S_{aij}} ln\left(\frac{r_m}{r_0}\right) \quad (r \le r_m) \\ S_{ji1}(z) &= \frac{r_0\tau_{j0}}{G_s}\frac{r_0}{S_{aij}} ln\left(\frac{r_m}{S_{aij}}\right) \quad (r \le r_m) \end{aligned}\right\} \tag{11}$$

Thus, under this working condition, after fully considering the reinforcement effect and shadowing effect of pile i on pile j, the actual displacement field induced by pile j is given by:

$$S^*_{jj}(z) = S_{jj}(z) - S_{ji}(z) = \frac{r_0\tau_{j0}}{G_s} ln\left(\frac{r_m}{r_0}\right) - \frac{r_0\tau_{j0}}{G_s}\cdot\frac{r_0}{S_{aij}} ln\left(\frac{r_m}{S_{aij}}\right) \tag{12}$$

Similarly, the actual deformation field of pile i is given by:

$$S^*_{ij}(z) = S_{ij}(z) - S^*_{ij1}(z) = \frac{r_0\tau_{j0}}{G_s} ln\left(\frac{r_m}{S_{aij}}\right) - \frac{r_0\tau_{j0}}{G_s}\cdot\frac{r_0}{S_{aij}} ln\left(\frac{r_m}{r_0}\right) \tag{13}$$

Based on the definition of the interaction coefficient, the subsequent expressions can be derived from formulas (12) and (13):

$$\xi_{ij} = \frac{S^*_{ij}(z)}{S^*_{jj}(z)} = \frac{\frac{r_0\tau_{j0}}{G_s}\left[ln\left(\frac{r_m}{S_{aij}}\right) - \frac{r_0}{S_{aij}} ln\left(\frac{r_m}{r_0}\right)\right]}{\frac{r_0\tau_{j0}}{G_s}\left[ln\left(\frac{r_m}{r_0}\right) - \frac{r_0}{S_{aij}} ln\left(\frac{r_m}{S_{aij}}\right)\right]} = \frac{ln\left(\frac{r_m}{S_{aij}}\right) - \frac{r_0}{S_{aij}} ln\left(\frac{r_m}{r_0}\right)}{ln\left(\frac{r_m}{r_0}\right) - \frac{r_0}{S_{aij}} ln\left(\frac{r_m}{S_{aij}}\right)} \quad (r \le r_m) \tag{14}$$

By introducing the interaction coefficient, formula (1) is transformed into:

$$\begin{aligned} S_i(z) &= S^*_{ii}(z) + \sum_{j=1,j\neq i}^{n} S^*_{ij}(z) = S^*_{ii}(z) + \sum_{j=1,j\neq i}^{n} \xi_{ij} S^*_{jj}(z) \\ &= S^*_{ii}(z) + \sum_{j=1,j\neq i}^{n} \frac{ln\left(\frac{r_m}{S_{aij}}\right) - \frac{r_0}{S_{aij}} ln\left(\frac{r_m}{r_0}\right)}{ln\left(\frac{r_m}{r_0}\right) - \frac{r_0}{S_{aij}} ln\left(\frac{r_m}{S_{aij}}\right)} S^*_{jj}(z) \end{aligned} \tag{15}$$

3. Deformation Calculation of Two Loading Conditions

3.1. S^*_{ii} Calculation

Under the loading condition where "pile j is present with no load on its top, and the load on the top of pile i is P_i", the lateral frictional resistance of the soil around pile i at a depth of z is $\tau_{i0}(r_0)$. The deformation field induced by $\tau_{i0}(r_0)$ at a depth of z is as follows:

$$\left.\begin{aligned} S_{ii}(z) &= \frac{\tau_{i0} r_0}{G_s} ln\left(\frac{r_m}{r}\right) \quad (r < r_m) \\ S_{ii}(z) &= 0 \quad (r \ge r_m) \end{aligned}\right\} \tag{16}$$

According to the shear deformation mechanism of coaxial cylindrical shells, the frictional resistance $\tau_{i0}(r_0)$ of the soil surrounding pile i is transmitted in the form of shear stress in the radial direction. At the same depth of pile j:

$$\tau_{ji} = \frac{\tau_{i0} r_0}{S_{aij}} \tag{17}$$

In the formula above, the τ_{ji} is the side friction resistance of pile j caused by pile i. At this point, the pile j will generate an equal and opposite amount of side friction resistance τ_{ji}^*. Substituting the formula (17) into the formula (16), the deformation field of the soil surrounding pile i caused by τ_{ji}^* can be obtained:

$$\left.\begin{aligned} S_{ij1}(z) &= \frac{r_0 \tau_{i0}}{S_{aij}} \cdot \frac{r_0}{G_s} ln\left(\frac{r_m}{r}\right) \quad (r < r_m) \\ S_{ij1}(z) &= 0 \quad (r \geq r_m) \end{aligned}\right\} \tag{18}$$

Taking into account the RSE between pile i and pile j, the deformation at a depth of z at the location of pile i induced by P_i is as follows:

$$S_{ii}^*(z) = S_{ii}(z) - S_{ij1}(z) = \frac{\tau_{i0} r_0}{G_s}\left[ln\left(\frac{r_m}{r}\right) - \frac{r_0}{S_{aij}} ln\left(\frac{r_m}{S_{aij}}\right)\right] \tag{19}$$

Based on formula (19), the equivalent spring stiffness of the pile-soil system for pile i can be formulated as:

$$k_{sii} = \frac{2\pi G_s}{ln\left(\frac{r_m}{r_0}\right) - \frac{r_0}{S_{aij}} ln\left(\frac{r_m}{S_{aij}}\right)} \tag{20}$$

The governing differential equation for pile i is presented below:

$$E_p A_p \frac{d^2 S_{ii}^*(z)}{dz^2} - k_{sii} S_{ii}^*(z) = 0 \tag{21}$$

Based on the loading condition where "pile j is present with no load on its top, and the load on the top of pile i is P_i", the boundary conditions for formula (21) are as follows:

$$\left.\begin{aligned} E_p A_p \frac{dS_{ii}^*(z)}{dz}\Big|_{z=0} &= P_i \\ E_p A_p \frac{dS_{ii}^*(z)}{dz}|_{z=l} &= -k_b S_{ii}^*(z)|_{z=l} \end{aligned}\right\} \tag{22}$$

For pile i , the expression for the equivalent stiffness coefficient of the soil at its pile tip is [32]:

$$k_b = \frac{8\pi E_s (1-\nu_s)}{(1+\nu_s)(k_1+k_2)} \tag{23}$$

where $k_1 = \frac{3(3-4\nu_s)}{2r_0} + \frac{8(1-\nu_s)^2 - (3-4\nu_s)}{\left(4r_0^2/9 + 4l^2\right)^{1/2}}$, $k_2 = \frac{2l^2(5-8\nu_s)}{\left(4r_0^2/9+4l^2\right)^{3/2}} + \frac{24l^2}{\left(4r_0^2/9+4l^2\right)^{5/2}}$.

By solving the above Equations (21) and (22):

$$S_{ii}^*(z) = c_1 e^{\lambda_{ii} z} + c_2 e^{-\lambda_{ii} z} \tag{24}$$

where $\lambda_{ii} = \sqrt{\frac{k_{sii}}{E_p A_p}}$, $k_{sii} = \frac{2\pi G_s}{ln\left(\frac{r_m}{r_0}\right) - \frac{r_0}{S_{aij}} ln\left(\frac{r_m}{S_{aij}}\right)}$, $c_1 = \frac{P_i e^{-\lambda_{ii} l}(1 - k_b \lambda_{ii}/k_{sii})}{2\left[E_p A_p \lambda_{ii} \sinh(\lambda_{ii} l) + k_b \cosh(\lambda_{ii} l)\right]}$,

$c_2 = \frac{P_i e^{\lambda_{ii} l}(1 + k_b \lambda_{ii}/k_{sii})}{2\left[E_p A_p \lambda_{ii} \sinh(\lambda_{ii} l) + k_b \cosh(\lambda_{ii} l)\right]}$.

3.2. S_{jj}^* Calculation

In the same way, under the loading condition where "pile i is present with no load on its top, and the load on the top of pile j is P_j", the actual deformation of pile j that takes into account the mutual RSE between pile i and pile j is as follows:

$$S_{jj}^*(z) = c_3 e^{\lambda_{jj} z} + c_4 e^{-\lambda_{jj} z} \tag{25}$$

where $\lambda_{jj} = \sqrt{\frac{k_{sjj}}{E_p A_p}}$, $k_{sjj} = \frac{2\pi G_s}{\ln\left(\frac{r_m}{r_0}\right) - \frac{r_0}{S_{aij}} \ln\left(\frac{r_m}{S_{aij}}\right)}$, $c_3 = \frac{P_j e^{-\lambda_{jj} l}\left(1 - k_b \lambda_{jj} / k_{sjj}\right)}{2\left[E_p A_p \lambda_{jj} \sinh(\lambda_{ii} l) + k_b \cosh(\lambda_{jj} l)\right]}$,

$c_4 = \frac{P_j e^{\lambda_{jj} l}\left(1 + k_b \lambda_{jj} / k_{sjj}\right)}{2\left[E_p A_p \lambda_{jj} \sinh(\lambda_{jj} l) + k_b \cosh(\lambda_{jj} l)\right]}$.

3.3. Deformation Analytical Solutions of Pile Group

Taking into account the mutual RSE between pile i and pile j, the final deformation of pile i can be obtained by the formula (15):

$$\begin{aligned} S_i(z) &= S_{ii}^*(z) + \sum_{j=1, j\neq i}^{n} S_{ij}^*(z) = S_{ii}^*(z) + \sum_{j=1, j\neq i}^{n} \xi_{ij} S_{jj}^*(z) \\ &= S_{ii}^*(z) + \sum_{j=1, j\neq i}^{n} \frac{ln\left(\frac{r_m}{S_{aij}}\right) - \frac{r_0}{S_{aij}} ln\left(\frac{r_m}{r_0}\right)}{ln\left(\frac{r_m}{r_0}\right) - \frac{r_0}{S_{aij}} ln\left(\frac{r_m}{S_{aij}}\right)} \end{aligned} \tag{26}$$

Given that the downward compressive load P on the top of the pile cap is ascertained, and assuming the pile cap is a flexible platform, the deformation of the pile can be calculated using the following equations($S_{aij} \le r_m$):

$$\left.\begin{aligned} P_i &= \frac{P}{n} \quad (1 \le i \le n) \\ z &= 0 \end{aligned}\right\} \tag{27}$$

In the case of a rigid pile cap, the deformation of the pile can be determined by applying the following equations($S_{aij} \le r_m$):

$$\left.\begin{aligned} &S_i(z=0) = S_j(z=0) \quad (1 \le i \le n) \\ &\sum_{i=1}^{n} P_i = P \end{aligned}\right\} \tag{28}$$

4. Examples

4.1 Example 1

The Plum Valley Bridge spans the valley of the Plum Valley, the bridge length is 1031.86m, the arrangement of spans is as follows: 7×32m prestressed concrete beams, (72+3×128+72) m prestressed concrete continuous rigid frame composite system, and 8×32m prestressed concrete beams. The main pier of the composite system is transverse circular arc hollow pier, the highest pier is $107m$. Due to the highly complex geological conditions at the site and the low bearing capacity of the soil and rock mass, the large friction pile group is adopted in the composite system, in which the pile number is 16~50, the pile length is 20m~40m, the maximum cap size is 18.1m×37.6m×5m.

Three artificial bored piles close to the bridge are chosen as prototype test piles. These piles have a diameter of 1.5m, and the concrete strength grade of the pile body is C20. The details of the test piles are as follows: The 10# pile cap has 50 piles with a length of 40 m; the 11# pile cap has 32 piles with a length of 37m; the 12# pile cap has 16 piles with a length of 28 m. The design parameters of the pile caps are presented in Table 1, and the layout of the pile foundation is shown

in Fig. 2. The relative elevation between 11# pile cap and 12# pile cap is 80m, and there are more than 70 meters of artificial slope. The maximum loading capacity of the test pile is 12824.70kN, and the test load is divided into 13 steps. The unloading load per level is twice of the load increment per level.

Table 1. Parameters of pile caps

Pile cap number	Number of piles	Pile length(m)	Pile diameter(m)	Pile spacing(m)	Size of pile cap(m3)	Strength grade of concrete
12# pile cap	4×4	28	1.50	3.90	14.2×14.2×4.0	C20
11# pile cap	4×8	37	1.50	3.90	14.2×29.8×5.0	C20
10# pile cap	5×10	40	1.50	3.90	18.1×37.6×5.0	C20

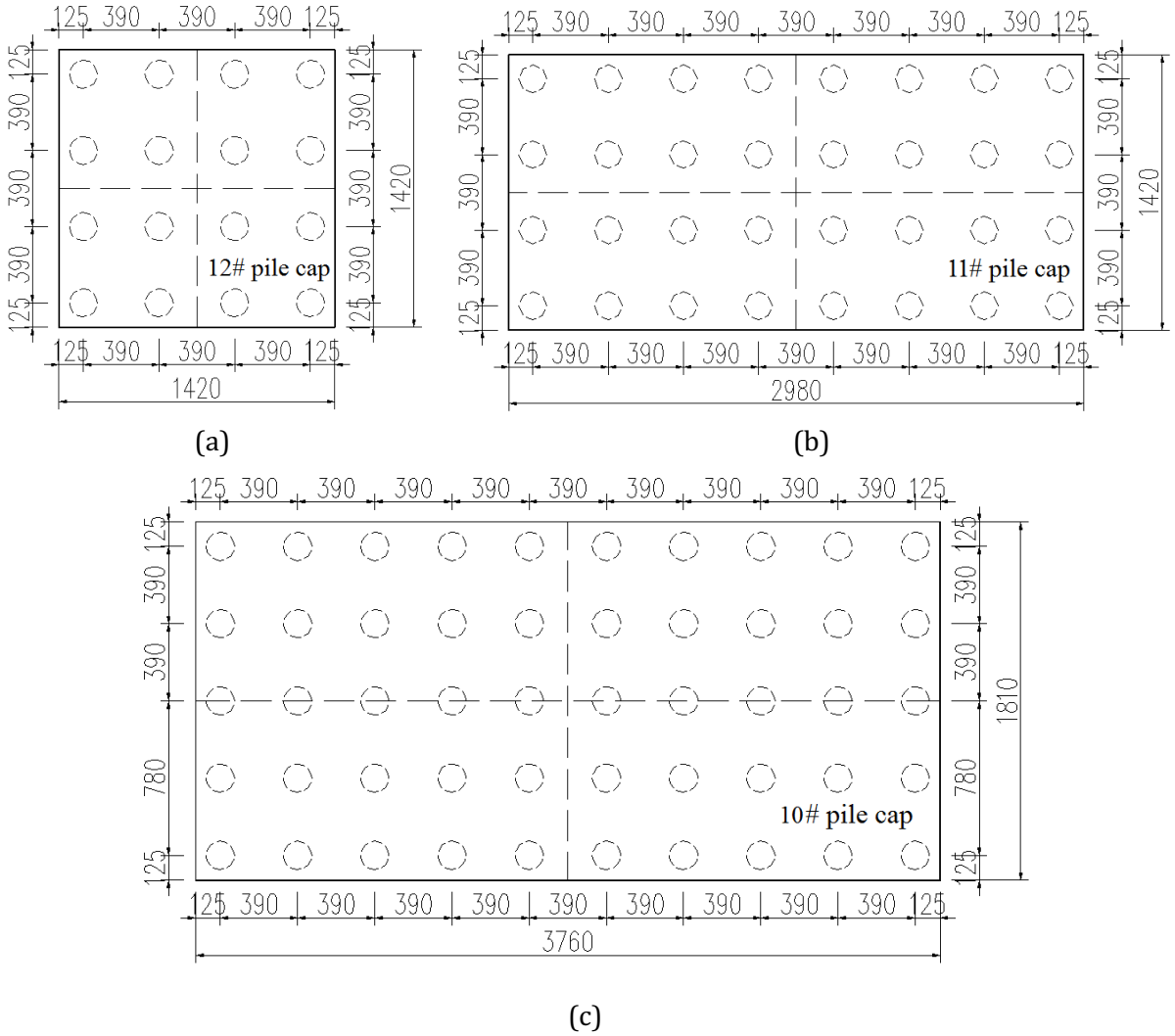


Fig. 2. Layout of pile foundation. (a) 12# pile cap; (b) 11# pile cap; (c) 10# pile cap

The bridge is situated in a tectonic erosion Canyon landform. Based on the geological survey report, the characteristic parameters of the soil-rock in the field pile group are listed in Table 2, where R_c, c, φ, and γ denote the uniaxial compressive strength, cohesion, internal friction angle, and bulk density of the soil (rock), respectively.

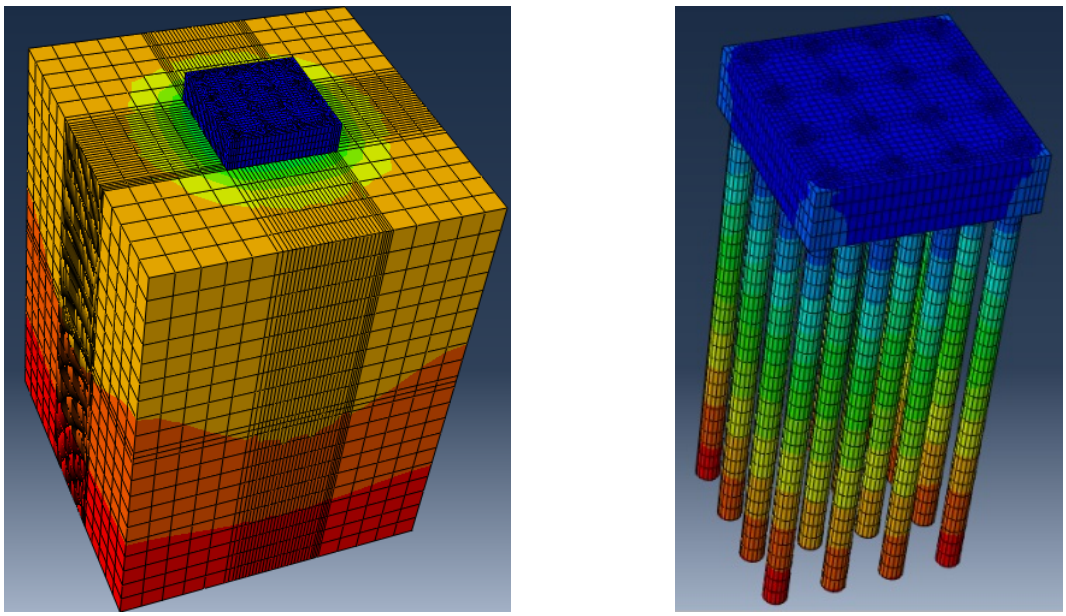
Table 2. Parameters of field rocks and soils

Name of soil layer	R_c(kPa)	c(kPa)	φ(0)	γ(kN/m^3)	Distribution layer thickness(m)
Sand clay	180	18	15	19	0~-10
Carbonaceous shale W2-1	350	—	40	23	-10~-30
Carbonaceous shale W2-2	400	—	45	24	-30~

Table 3. Calculation parameter values for rock and soil

Name of soil layer	E_s(MPa)	c(kPa)	φ(0)	υ_s	γ(kN/m^3)	Distribution layer thickness(m)
Sand clay	450	18	15	0.4	19	0~-10
Carbonaceous shale W2-1	4050	—	40	0.25	23	-10~-30
Carbonaceous shale W2-2	4500	—	45	0.25	24	-30~

Note: the thickness of the distribution layer is measured starting from the bottom of the pile cap.



(a) (b)

Fig. 3. Three-dimensional finite element analysis model. (a) Grid division; (b) Pile foundation and pile cap

Table 4. Deformation calculation results of test piles (mm)

Load (kN)	10# pile cap		11# pile cap		12# pile cap			
	δm	δc	δm	δc	δm	δc	δf	δp
986.52	0.170	0.181	0.010	0.015	0.180	0.186	0.183	0.298
1973.04	0.288	0.302	0.085	0.088	0.380	0.387	0.384	0.424
2959.56	0.493	0.501	0.197	0.202	0.575	0.581	0.576	0.614
3946.48	0.685	0.693	0.312	0.327	0.790	0.807	0.802	0.983
4932.60	0.903	0.940	0.432	0.439	0.973	1.021	0.992	1.236
5919.12	1.224	1.285	0.572	0.583	1.293	1.305	1.301	1.438
6905.64	1.536	1.573	0.735	0.742	1.488	1.492	1.494	1.674
7892.16	1.856	1.872	0.858	0.862	1.758	1.762	1.776	1.849
8878.68	2.209	2.231	0.978	0.993	2.108	2.210	2.239	2.405
9865.20	2.573	2.586	1.109	1.112	2.320	2.431	2.576	2.714
10851.72	2.944	2.992	1.273	1.284	2.675	2.708	2.873	3.015
11838.24	3.329	3.411	1.443	1.531	2.950	3.041	3.254	3.838
12824.70	3.739	3.757	1.632	1.732	3.410	3.562	3.793	4.298

Note: δ_m, δ_c, and δ_f represent the measured deformation, the theoretical calculation value, and the results of FEM, respectively; δ_p denotes the result calculated via Poulos's elastic theory method [18,19].

To compare the finite element calculation results with the theoretical and field test results, a numerical simulation of the 12# pile cap is conducted. The finite element model is illustrated in Fig. 3. The pile cap and piles have a strength grade of C20, with an elastic modulus E_p=25.5GPa, a Poisson's ratio of 0.17, and a bulk density γ=25 kN/m^3. The calculation parameters for the theoretical and finite element methods are presented in Table 3, where E_s,、 c、 φ、 υ_s、 γ denote the modulus, cohesion, internal friction angle, Poisson's ratio, and bulk density of the rock and soil, respectively. In theoretical analysis, the pile cap is typically assumed to be rigid. In practice, when a pile cap satisfies the punching shear strength requirements, its behavior generally approximates that of a rigid plate [29,32]. The calculation results are shown in Table 4.

A comprehensive evaluation of the test and computational data presented above yields the following findings:

- Theoretically calculated deformation values are observed to be marginally higher than the measured values, with the discrepancy remaining within a relatively confined range (typically not exceeding 10%). This phenomenon is attributed to the assumption of pile-tip elasticity [32] used in deriving the theoretical model, which introduces a degree of conservatism when calculating pile-tip settlement. However, the overall deviation is negligible, suggesting that the model's conservatism remains within an acceptable range for engineering applications. In addition, the settlement results calculated by Poulos's elastic theory method (δp) are generally larger than the measured values, the simplified theoretical values and the finite element results, showing relatively obvious deviation from the measured deformation data.
- The pile-soil system exhibits elastic behavior during the initial four to five load levels, a phenomenon referred to as the elastic stage. At this stage, the discrepancy between the theoretical and measured values is negligible. Concurrently, the FEM calculation results demonstrate a substantial degree of concordance with the measured values. There is virtually no discernible difference among the three, indicating the consistency of the theoretical method, numerical method, and measured results during the elastic stage; the RSE theoretical model demonstrates excellent applicability in the elastic stage. By contrast, the settlement values solved by Poulos's elastic theory deviate visibly from the test measurements even in the elastic loading phase.
- As the load level increases, the soil transitions to the elastoplastic stage, and the finite element calculation results become increasingly aligned with the measured values, particularly at maximum load (12824.70 kN). The discrepancy between the FEM result of 3.793 mm for Pile Cap No. 12 and the measured value of 3.410 mm is less significant than the discrepancy between the theoretical value of 3.562 mm and the measured value. The Poulos elastic theory yields a calculated settlement of 4.298 mm under the maximum load, which produces the largest deviation from the measured value among all computational methods. This comparison highlights the notable advantages of the finite element method in considering material nonlinearity and interfacial contact nonlinearity of the pile-soil system. Meanwhile, it indirectly verifies that the rational selection of geotechnical parameters (especially soil nonlinear parameters) can greatly improve the accuracy of numerical calculation.

4.2 Example 2

To investigate the compressive bearing characteristics of pile group with rigid pile caps, a series of model tests were conducted in soft soil and silt soil foundations respectively [34]. In the soft soil scenario, the model piles were made of seamless steel pipes with a specification of ϕ100mm × 4mm. The elastic modulus of the model piles was set at 2.1×10^5MPa, and the bottoms of the model piles were welded to tapered head plates. The model piles were pre-drilled before being driven by the static pressure method. The soil conditions of the foundation were as follows: the soil above a depth of 4.0m was soft- plastic silty clay, and the soil below 4.0m was soft-plastic muddy silty clay. The soil parameters used for the deformation calculation of the pile group model in the soft soil foundation were: a shear modulus of 3MPa and a Poisson's ratio of 0.35. In the silt soil, the model piles were similar to the engineering prototype piles. A series of tests with varying design

parameters (pile length, pile diameter, pile spacing) were carried out within the range of the bearing capacity eigenvalues of the pile group model ($P \leq P_u/2$, where P_u is the standard value of the ultimate bearing capacity of the pile group model). The soil conditions of the silt foundation were: the soil above a depth of 8.0m was slightly compacted~medium dense silt soil, and the soil below 8.0m was plastic~soft plastic silty clay. The soil parameters for the deformation calculation of the pile group model in the silt soil foundation were: an elastic modulus of the model pile of 2.0×10^4MPa, a soil shear modulus of 8MPa, and a Poisson's ratio of 0.30. In this example, the deformation of the pile group model calculated by the theoretical method of this paper was compared with that obtained by the method of the Technical Code for Building Pile Foundations (JGJ94 - 2008) [17] and the method proposed by Zhao et al [34]. The results are presented in Table 5.

Table 5. Deformation calculation results of pile group (mm)

Soil type	silt soil				soft soil
Numbering	G11	G16	G17	G18	G9B
d(mm)	330	250	250	250	100
l/d	14	18	18	18	45
S_a/d	3	3	4	6	4
n	3×3	3×3	3×3	3×3	4×4
Measured value S(mm)	6.0	4.1	3.2	3.4	2.8
Method specified in GB 50007 S_2(mm)	6.7	4.7	4.0	3.7	3.1
Method of Zhao et al. S_1(mm)	8.2	7.8	5.2	3.9	4.4
Proposed method S_3(mm)	6.4	4.5	3.8	3.7	2.9
S_2/S	1.12	1.15	1.25	1.09	1.11
S_3/S	1.07	1.10	1.19	1.09	1.04

Analysis of the calculated and tested results reveals the following:

- The pile-group deformation derived from the theoretical method is close to the measured deformation, yet slightly larger than the experimental deformation. The primary reason for this discrepancy is that the pile-end deformation is calculated using solutions of elasticity theory [31,32].
- The pile-group deformation obtained by the theoretical method proposed in this paper is smaller than that calculated in accordance with the current Chinese national code Technical Code for Building Pile Foundations (JGJ 94-2008) [17]. The reason is that the current Chinese national code adopts the layered summation method based on the equivalent pier foundation assumption, and fails to consider the RSE among piles within the pile group.
- It is evident that the interaction coefficient for pile-to-pile interaction within the pile group, introduced in this paper, overcomes the limitations of existing methods, which either fail to consider or do not adequately account for the mutual RSE of piles [32]. The theoretical method proposed in this paper aligns with the actual engineering characteristics of pile group.

5. Analysis of Influencing Factors Based on RSE

Numerous studies [2,4,6,9,32] have shown that the deformation of pile group is controlled not only by the load, pile geometric and material parameters, but also significantly affected by the internal RSE within the pile group. Main influencing factors include: the total load P, pile length l, pile radius r_0, pile spacing S_{aij}, elastic modulus of the pile body E_p, shear modulus G_s(alternatively,E_s can be used, with the conversion relation $E_s=2(1+\nu_s)G_s$), and soil Poisson's ratio ν_s. For a pile-group foundation with a specific number of piles, the relationship governing the pile-group deformation can be expressed as:

$$S_G = f_1(P, S_{aij}, r_0, l, G_s, E_p, v_s) \tag{29}$$

in the above formula, the dependent variables and the respective variables are expressed as:

$$L, MLT^{-2}, L, L, L, ML^{-1}T^{-2}, ML^{-1}T^{-2}, 0 \tag{30}$$

After the dimensional analysis, there are two independent dimensions in the above formula, namely L and MT^{-2}. Here, using r_0 to eliminate the dimensional L, and using G_s to eliminate the dimensional MT^{-2}, which can be obtained:

$$\frac{S_G}{r_0} = f_2\left(\frac{P}{G_s r_0^2}, \frac{l}{r_0}, \frac{S_{aij}}{r_0}, \frac{E_p}{G_s}, v_s\right) \tag{31}$$

In the elastic working state, the deformation is proportional to the load, so the formula above can be converted to:

$$\frac{1}{P/G_s r_0 S_G} = f_3\left(\frac{1}{r_0}, \frac{S_{aij}}{r_0}, \frac{E_p}{G_s}, v_s\right) \tag{32}$$

where the physical meaning of $P/(G_s r_0 S_G)$ can be understood as the deformation stiffness parameter of pile group.

According to the theoretical calculation method of pile group deformation proposed in this paper, we assume that there is a pile group (rectangular layout of 3 × 3) in homogeneous soil, and based on the assumption above, the influence research of length-diameter ratio l/r_0, spacing-diameter ratio S_{aij}/r_0, pile-soil modulus ratio E_p/G_s and Poisson's ratio of soil υ_s on deformation stiffness parameter of pile group $P/(G_s r_0 S_G)$ is carried out. In the calculation, the pile cap is assumed to be completely rigid, of course, it can also assume fully flexible. In the actual project, when the pile cap meets the pile's anti punching and bending strength condition, the pile cap is closed to the rigid assumption in ordinary circumstances.

5.1. Length-Diameter Ratio

When the pile spacing $S_{\alpha ij} = 5r_0$, the pile-soil modulus ratio $E_P/G_s = 5000$, and the soil Poisson's ratio υ_s= 0.40, the relationship between the stiffness parameter of the pile group $P/(G_s r_0 S_G)$ and the length-diameter ratio l/r_0 is illustrated in Fig. 4.

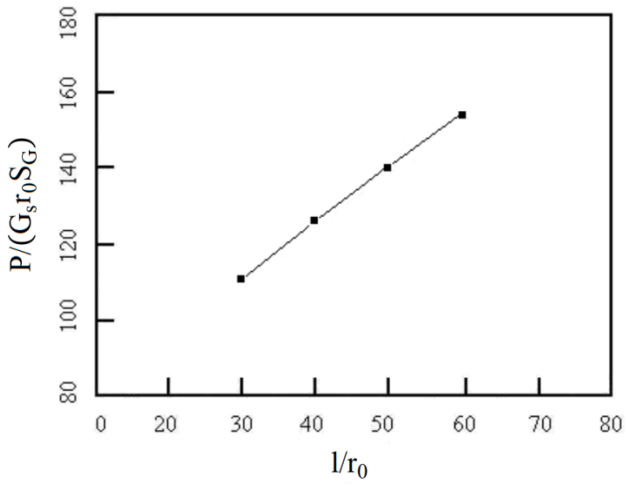


Fig. 4. Effect of l/r_0 on S_G

As shown, $P/(G_s r_0 S_G)$ rises as the length-diameter ratio l/r_0 increases. That is, when the pile diameter r_0 remains constant, an increase in pile length l can effectively enhance the pile group's resistance to deformation. When the pile length l is unchanged, increasing the pile diameter r_0 can boost the pile group's deformation resistance. This is because for the same pile length, the pile-side area and pile body stiffness increase with an increase in pile diameter r_0. In other words, when other influencing factors are fixed, the pile group deformation S_G decreases as l/r_0 increases, and an increase in pile length l is beneficial for increasing the bearing capacity and reducing the

deformation of the pile foundation. The reason is that RSE affects the superposition of soil stress, and thereby amplifies or weakens the additional deformation effect of RSE. Therefore, in the design of compressive pile group under specific geological conditions, when the pile diameter of the group satisfies the checks for compressive strength, bearing capacity of the pile group, and allowable deformation of the pile group, conducting computational analysis and selecting a length-diameter ratio l/r_0 suitable for the actual engineering requirements serves as a measure for optimizing the design of compressive pile group.

5.2. Spacing-Diameter Ratio

When the pile length $l = 30r_0$, the pile-soil modulus ratio $E_P/G_s = 5000$, and the soil Poisson's ratio υ_s= 0.40, the relationship between the stiffness parameter of the pile group $P/(G_s r_0 S_G)$ and the spacing-diameter ratio S_{aij}/r_0 is shown in Fig. 5.

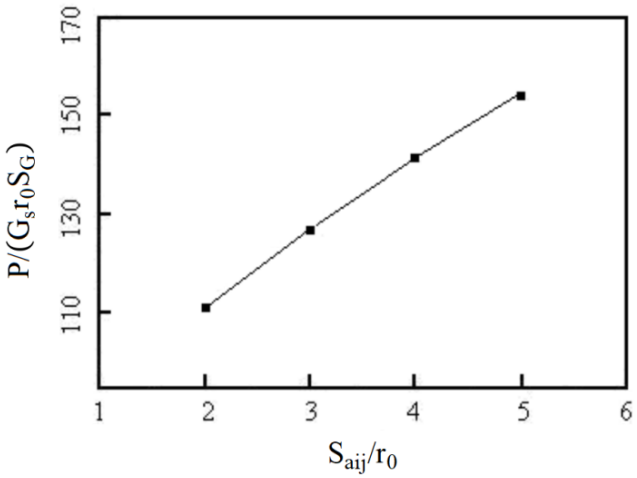


Fig. 5. Effect of S_{aij}/r_0 on S_G

As can be observed, $P/(G_s r_0 S_G)$ increases as the spacing-diameter ratio S_{aij}/r_0 grows, indicating that the pile group's resistance to deformation is enhanced. When other influencing factors are fixed, the pile group deformation S_G decreases with an increase in the spacing-diameter ratio S_{aij}/r_0. This is because a larger pile spacing S_{aij} weakens the mutual RSE among piles in the pile group. Consequently, in the design of pile group, when engineering conditions allow, besides increasing the length-diameter ratio l/r_0 to control pile group deformation S_G, increasing the spacing-diameter ratio S_{aij}/r_0 is also an effective measure.

5.3. Pile-Soil Modulus Ratio

When the pile spacing $S_{aij} = 5r_0$, pile length $l = 30r_0$, and soil Poisson's ratio υ_s =0.40, the relationship between the stiffness parameter of the pile group $P/(G_s r_0 S_G)$ and the pile-soil modulus ratio E_p/G_s is presented in Table 6.

Table 6. Calculation parameter values for rock and soil

E_p/G_s	150	400	800	3000
$P/(G_s r_0 S_G)$	74.3	98.1	103.6	126.8

Analyzing the data, it can be seen that $P/(G_s r_0 S_G)$ increases as the pile-soil modulus ratio E_p/G_s rises. This implies that the pile group's resistance to deformation is enhanced. Therefore, increasing the strength grade of concrete or the amount of concrete reinforcing bars can improve the pile group's ability to resist deformation. The reason is that in soft soil, the greater the pile stiffness, the more significant the contribution of the pile-pile RSE in the pile group to deformation resistance. However, as E_p/G_s increases (with the pile being considered infinitely rigid relative to the soil), the impact of E_p/G_s on $P/(G_s r_0 S_G)$ significantly diminishes according to the calculation results. Thus, simply increasing the pile strength yields limited effects at this stage; it is more

advisable to improve the soil properties around the pile through measures such as pile end grouting and pile side reinforcement.

6. Conclusions

This study has delved into the deformation calculation of compressive pile groups with consideration of RSE. A novel analytical method, which aligns with the synergistic working behaviour of pile groups in actual projects, has been proposed and employed for case analysis and parameter investigation. The main conclusions obtained in this study are as follows:

- In view of the deficiency that existing research fails to distinguish the bidirectional RSE among piles, this study redefines the concept of RSE for pile groups. Unlike existing interaction-factor methods that treat pile-pile interaction as a unidirectional displacement superposition, the proposed method, based on the shear deformation mechanism of coaxial cylindrical shells, establishes an analytical framework that simultaneously captures both the reinforcement and shadowing components. The introduced pile-pile interaction coefficient ξij provides a mechanistic rather than empirical quantification of RSE, alleviating key limitations of conventional analytical frameworks in reflecting the actual mechanical response of pile groups.
- The theoretical calculation method for pile group deformation considering the RSE proposed in this paper shows a high consistency between the calculated results and measured values in the elastic working stage, which verifies the accuracy and reliability of the method and can be directly applied to the prediction of pile foundation deformation in engineering design. Meanwhile, the theoretical calculated values are slightly larger than the measured ones, indicating that the calculation model possesses a certain degree of conservatism, which is more conducive to ensuring engineering safety.
- By adopting the proposed theoretical method, the influencing factors based on the RSE of pile group are analyzed. The results show that the length-diameter ratio, spacing-diameter ratio, pile-soil modulus ratio all affect the deformation stiffness of pile group by changing the pile-pile RSE. Increasing the length-diameter ratio and reasonably enlarging the spacing-diameter ratio can enhance the RSE and improve the deformation resistance of pile group. Simply increasing the pile modulus has a limit in characterizing the RSE, and improving the soil properties around piles is the fundamental way to regulate the RSE and optimize the deformation performance of pile group.
- The proposed theoretical method exhibits good applicability to pile group with different pile layout forms and under various load levels, and is particularly suitable for the rapid deformation analysis of large-scale pile groups. Comparison with finite element calculation results shows that the method achieves reliable calculation accuracy in the elastic stage with higher computational efficiency, making it more convenient for popularization and application in practical engineering.
- Further research can couple the theoretical model in this study with the algorithm considering pile-soil nonlinearity. On the premise of guaranteeing computational efficiency, the calculation accuracy under high load levels can be further improved, providing a more comprehensive theoretical support for the deformation calculation of pile group under various construction conditions and geological environments.

Nomenclature

The following symbols are used in this article:

A_p = Cross-sectional area of the pile;
E_p = Elastic modulus of the pile;
E_s = Elastic modulus of the soil;
G_s = Shear modulus of the soil;
l = Embedment depth of the pile;
k_b = Equivalent stiffness coefficient of pile-tip soil;
k_s = Equivalent spring stiffness of pile-soil system;

P = Load;
r = Distance from the pile's axis (horizontal);
r_0 = Pile radius;
r_m = Influence radius of shear deformation;
S = Pile shaft deformation;
S_a = Axial distance between piles;
v_p = Poisson's ratio of the pile;
v_s = Poisson's ratio of the soil;
ξ = Pile-pile interaction coefficient;
τ = Lateral frictional resistance.

Acknowledgement

The research reported in this study was supported by the Scientific and Technological Innovation Project of Zhejiang Guangsha Vocational and Technical University of Construction (Grant No. 2024ZX115). The authors appreciate the critical comments and valuable suggestions from the anonymous reviewers, which greatly improved the manuscript.

References

[1] Dai G, Dai Y, Liu Y, Gong W. Study of pile group effect coefficient for super-long bored piles. China Civ Eng J. 2011;44(10):107-112. https://doi.org/10.15951/j.tmgcxb.2011.10.012
[2] Ukritchon B, Faustino JC, Keawsawasvong S. Numerical investigations of pile load distribution in pile group foundation subjected to vertical load and large moment. Geomech Eng. 2016;10(5):577-598. https://doi.org/10.12989/gae.2016.10.5.577
[3] Liu SW, Zhang QQ, Cui CY, Feng RF, Cui W. A simplified approach for the response of pile groups composed of dissimilar piles. Structures. 2021;34:4548-4559. https://doi.org/10.1016/j.istruc.2021.10.063
[4] Junior EC, Moura AS. Evaluation of the group effect's simulation on the bearing capacity of bored piles in granular soil, using load transfer functions. Geotech Geol Eng. 2022;40(6):3393-3412. https://doi.org/10.1007/s10706-022-02100-1
[5] Yigit MA, Onur MI, Balaban E. Investigation of soil pile interaction parameters in piled foundations. J Fac Eng Archit Gazi Univ. 2022;37(2):625-639. https://doi.org/10.17341/gazimmfd.825224
[6] Mishra A, Venkatesh K, Karumanchi SR. 3D numerical analysis of single pile and pile-raft subjected to vertical loading. Indian Geotech J. 2023;53(3):686-697. https://doi.org/10.1007/s40098-022-00707-y
[7] Chiang KH, Hung WY, Tran MC, Ha TQ. The vertical loading tests of single and group piles by centrifuge modelling. Int J Geotech Eng. 2024;18(6):537-553. https://doi.org/10.1080/19386362.2024.2376532
[8] Khatti J, Samadi H, Grover KS. Estimation of settlement of pile group in clay using soft computing techniques. Geotech Geol Eng. 2024;42(3):1729-1760. https://doi.org/10.1007/s10706-023-02643-x
[9] Li K, Chen S, Zhao P, Pei R. Theoretical and numerical simulation analysis of the control effect of isolation piles on surface settlement induced by foundation pit excavation. Geomech Eng. 2024;39(3):227-240. https://doi.org/10.12989/gae.2024.39.3.227
[10] Poulos HG. On the equivalent pier approximation for pile groups and piled rafts. Geotech Geol Eng. 2024;42(6):5269-5281. https://doi.org/10.1007/s10706-024-02840-2
[11] Chen YF, Ai ZY, Ma ZG, Ye ZK. Interaction between layered saturated soft rock-soil mass and pile groups considering free-standing length and rock-socketed depth. Int J Numer Anal Meth Geomech. 2025;49(12):2805-2819. https://doi.org/10.1002/nag.4014
[12] Della Corte A, Iodice C, Tsikas A, François S, Anoyatis G. An analytical approach to pile-to-pile interaction for end-bearing piles. Géotechnique. 2026;76(2):247-258. https://doi.org/10.1680/jgeot.24.01159
[13] Sandeep GS, Arun KYM, Pandit P, Alexander VB. Effect of soil-pile interaction on inclined pile group subjected to axial and lateral loads. Eng Lett. 2025;33(7):2713-2722.
[14] Siemaszko P. Pile-soil interaction during static load test. Stud Geotech Mech. 2024;46(3):164-175. https://doi.org/10.2478/sgem-2024-0010
[15] Wang T, Zhao Z, Chu Z, Wang X. Improved method for calculating settlement of pile foundations and case studies. Chin J Geotech Eng. 2023;45(11):2227-2237. https://doi.org/10.11779/CJGE20221011
[16] Zhang W, Shi J, Lin G, Lin C. Settlement analysis of a large pile group supporting an LNG storage tank. Int J Numer Anal Meth Geomech. 2025;49(16):3858-3879. https://doi.org/10.1002/nag.70052
[17] Ministry of Housing and Urban-Rural Development of the People's Republic of China. Technical Code for Building Pile Foundations: JGJ 94-2008. Beijing: China Architecture & Building Press; 2008.
[18] Poulos HG, Davis EH. Pile foundation analysis and design. New York: John Wiley & Sons; 1980.

[19] Poulos HG. Analysis of the settlement of pile groups. Géotechnique. 1968;18(4):449-471. https://doi.org/10.1680/geot.1968.18.4.449
[20] Randolph MF, Wroth CP. Analysis of the vertical deformation of pile groups. Géotechnique. 1979;29(4):423-439. https://doi.org/10.1680/geot.1979.29.4.423
[21] Davies TG, Gao XW. Three-dimensional elasto-plastic analysis via the boundary element method. Comput Geotech. 2006;33(3):145-154. https://doi.org/10.1016/j.compgeo.2006.03.003
[22] Beer G, Duenser C. Advanced boundary element analysis of geotechnical problems with geological inclusions. Comput Geotech. 2016;79:86-95. https://doi.org/10.1016/j.compgeo.2016.06.004
[23] Guo N, Zhao J. Multiscale insights into classical geomechanics problems. Int J Numer Anal Methods Geomech. 2016;40(3):367-390. https://doi.org/10.1002/nag.2406
[24] Liang WJ, Zhao JD. Multiscale modeling of large deformation in geomechanics. Int J Numer Anal Methods Geomech. 2019;43(5):1080-1114. https://doi.org/10.1002/nag.2921
[25] Prunier F, Branque D. Definition of a safety factor using the finite element method in geomechanics, from a static to dynamic regime. Eur J Environ Civ Eng. 2022;26(1):144-165. https://doi.org/10.1080/19648189.2019.1650119
[26] Chow YK. Analysis of vertically loaded pile groups. Int J Numer Anal Methods Geomech. 1986;10(1):59-72. https://doi.org/10.1002/nag.1610100105
[27] Shen WY, Chow YK, Yong KY. A variational approach for vertical deformation analysis of pile group. Int J Numer Anal Methods Geomech. 1997;21(11):741-752. https://doi.org/10.1002/(SICI)1096-9853(199711)21:11<741::AID-NAG898>3.0.CO;2-D
[28] Yao WJ, Chen SP. Elastic-plastic analytical solutions of deformation of uplift belled pile. Teh Vjesn. 2014;21(6):1201-1211.
[29] Yao WJ, Yuan CB, Chen SP. Analytical solutions of deformation of anti-pull group piles considering reinforcement effect. J Harbin Eng Univ. 2017;38(10):1573-1579. https://doi.org/10.11990/jheu.201605059
[30] Yao WJ, Xiao L. Analytical solutions of deformation of uplift belled group piles considering reinforcement effect. KSCE J Civ Eng. 2019;23(3):1007-1016. https://doi.org/10.1007/s12205-019-1635-4
[31] Xu JJ, Xu X, Yao WJ. New method for calculating the settlement of single pile and pile group in soft soil area. Adv Civ Eng. 2020;2020:8816704. https://doi.org/10.1155/2020/8816704
[32] Chen SP, Zheng YX, Zhou HC. Working performance and deformation theory of pile foundations under vertical and horizontal loads. Beijing: China Architecture & Building Press; 2026.
[33] Pandey G, Mourya VK, Patel D, Kumar R, Kumar S. Load sharing behaviour in piled-raft foundations over sand and clay: An experimental investigation. Res Eng Struct Mater. 2024;10(3):917-942. https://doi.org/10.17515/resm2023.41me0714rs
[34] Zhao MH, Zou D, Zou XJ. Settlement calculation of pile groups by load transfer method. Eng Mech. 2006;23(7):119-123. https://doi.org/10.3969/j.issn.1000-4750.2006.07.022